ESRF	**Experiment title:** Unveiling new boron-based 2D nanomaterials by synthesis in molten salts	**Experiment number:** MA-5188
Beamline: ID11	**Date of experiment:** 04/05/2022 – 10/05/2022	**Date of report:**
Shifts: 18	**Local contact(s):** Pierre-Olivier Autran pierre-olivier.autran@esrf.fr	*Received at ESRF:* 14/09/2022

Names and affiliations of applicants (*indicates experimentalists):
David Portehault,* Daniel Janisch,* Edouard de Rolland Dalon,* Isabel Gomez Recio,* Fernando Igoa*

Sorbonne Université, CNRS, Laboratoire de Chimie de la Matière Condensée de Paris (LCMCP), Paris, France

Introduction:
MBenes, or boridenes, are new 2D materials made of transition metals and boron, which attract huge interest for their expected electronic and catalytic properties.[1,2] The impact of MBenes on the science of 2D materials can be foreseen from the enthusiasm raised by their carbide and nitride analogues MXenes, where X = C or N respectively, and which are currently scrutinized for catalysis, magnetism, and energy storage.[3] MXenes are produced by chemical etching of MAX phases (A = metalloid), followed by exfoliation in the same medium,[4] usually aqueous hydrofluoric acid solutions. However, MAB phases are much less stable, hence such processes usually destroy the material[1] or incorporate large amounts of defects in the layers,[3] which impedes insights into the intrinsic properties of MBenes. The difficulty to exfoliate MAB phases lies in the M-B and M-A bond energy difference: M-B bonds are stronger than M-A ones but relatively close in energy,[3] which makes it difficult to find conditions to attack only the M-A bonds. Exfoliation thus requires prior production of pure MAB, and delamination in sufficiently soft conditions to avoid destroying the layered structure.

This experiment aimed at unveiling the mechanism and chemical conditions under which a selected MAB phase could be synthesized and delaminated: Fe_2AlB_2. Based on our previous experience and on recent literature reports, we proposed the hypothesis that both procedures (synthesis and delamination) could occur by assistance of a molten salt media. Therefore, we performed *in situ* time resolved X-ray diffraction to identify the adequate experimental parameters of synthesis and understand the evolution of layered materials into molten salts.

This proposal had two aims: (1) Identifying the ideal conditions of synthesis and exfoliation for a specific MAB phase: Fe_2AlB_2, which would yield an unreported 2D iron boride of large interest for electrocatalysis of hydrogen production from water and for ion batteries.[2] (2) Identifying and understanding by X-ray diffraction the process of exfoliation of Fe_2AlB_2 in molten salts.

Experimental:
For the experiment we employed a sample environment setup designed and developed within our group, that is, a capillary vertical oven. This oven has been designed to mimick lab syntheses, including handling of liquid media in an open vessel while flushing inert atmosphere in this vessel (capillary). The first shift of the experiment was dedicated to setting up the oven on the beamline (**Figure 1**) and adjusting the geometry of the hutch to the reach the *q* range required for the experiment. For further description on the *in situ* oven, the reader may refer to the experimental report of the MA-4760 experiment.

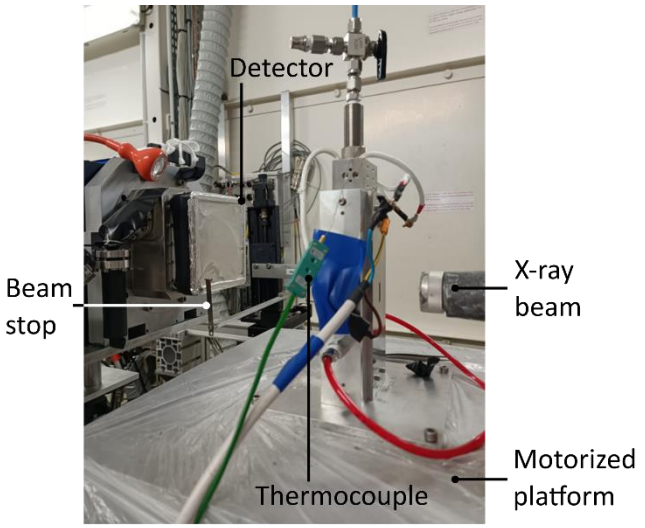

Figure 1. Sample environment mimicking for *in situ* synchrotron

After adjusting the analysis and detection conditions, the remaining shifts were dedicated to the analysis of reactions in molten salts. All of the experiments were performed at 10 °C·min^{-1} heating rate, which was identified as suitable to ensure crystallization to take place in the systems of interest in the lab. The capillaries were scanned continuously and diffractograms were acquired for 1 s at 10 vertical positions of the capillaries. Hence, for each position, a diffractometer was assessed every *ca*. 30 s. The experiments were performed with a variable dwell time depending on the specific reaction, which will be detailed for each case.

Results and discussion:

Fe_2AlB_2 can be synthesized from an elemental mixture (Fe + Al + B), but this usually requires long reaction times, temperatures and reproducibility is challenge. In contrast, its synthesis has also been realized from Al insertion into the FeB compound, which according to the literature renders much higher purity and reproducibility. The FeB compound however presents two structural modifications, a low temperature one that consists of an intergrowth of two structures (named α-FeB hereafter) and a high temperature modification (β-FeB), consisting of a classical periodic arrangement. The conditions of synthesis of Fe_2AlB_2 have not been explored, nor has the influence of the FeB polymorphism as starting material.

We firstly assessed the mechanism of transformation of α-FeB to Fe_2AlB_2 upon reaction with $NaAlCl_4$ and NaH as Al source and reducing agent, respectively. The diagrams are plotted against the reaction time as a heatmap in **Figure 2**. The low reagent's concentration in the media and the latter's diffuse scattering in the molten state limits the signal-to-noise ratio, but diffraction peaks are still observable. Interestingly, Al^0 formation is detected upon the disappearance of the NaH peaks at *ca*. 380 °C, when the salt completely melts. α-FeB remains up to ~ 845 °C, when the Fe_2AlB_2 peaks appear. The peak position mismatch to the reference is attributed to thermal dilatation. No signs of the characteristic reflections of β-FeB (absent in α-FeB) are detected, thus indicating a direct reaction from α-FeB to Fe_2AlB_2. These results support the hypothesis that Al^0 is firstly formed *in situ* throughout the reaction before being inserted inside α-FeB to yield Fe_2AlB_2, according to **Equations 1** and **2**, respectively. This is also in line with the fact that larger NaH excess rather than $NaAlCl_4$ excess leads to the completion of the reaction observed previously.

$$NaAlCl_4(s) + 3\ NaH(s) \rightarrow Al(s) + 4\ NaCl(s) + 1.5\ H_2(g) \qquad \textbf{Equation 1}$$

$$2\ \alpha\text{-}FeB(s) + Al(s) \rightarrow Fe_2AlB_2(s) \qquad \textbf{Equation 2}$$

β-FeB was reacted following the same protocol as the one optimized for α-FeB, that is FeB:$NaAlCl_4$:NaH = 2:3:10 with heating at 1000 °C for 1 h. The same *in situ* experiment starting from β-FeB (**Figure 3**) shows an identical reaction sequence, at similar temperatures. No important differences is observed between the products obtained by reaction of β-FeB and of α-FeB: both exhibit reflections of Fe_2AlB_2 as major phase, yet with a decrease in purity. α-FeB is an intergrowth of β-FeB and of CrB-type structures in a ratio ~1:1. Although α-FeB is nearly half-made of crystal domains that differ from β-FeB, no significant difference in reactivity is observed. We ascribe this behaviour to the important fraction of β-FeB domains (57%) in α-FeB, which ensure similar reactivity, especially topotactic transformation of the β-FeB domains into Fe_2AlB_2. Consequently, α-FeB, which requests much lower temperature of synthesis, can be used instead of β-FeB to produce Fe_2AlB_2 compound. Let it be noted that in the *in situ* scan of the β-FeB reaction, SiO_2 crystallization from the quartz capillary is observed at higher temperatures, which is an artefact due to interaction of the quartz capillary walls with NaH decomposition side-products.

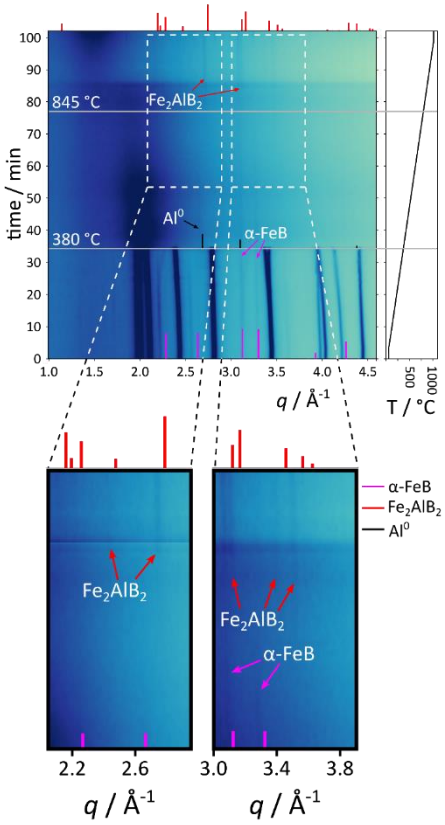

Figure 2. Synchrotron XRD *in situ* study of the α-FeB → Fe_2AlB_2 transformation.

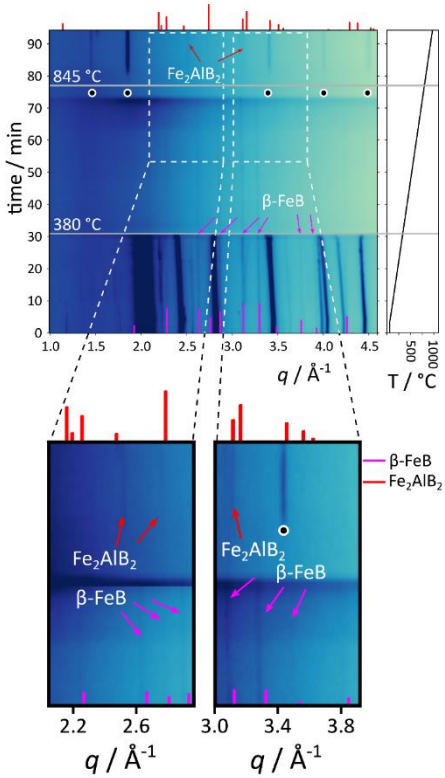

Figure 3. Synchrotron XRD *in situ* study of the β-FeB → Fe_2AlB_2 transformation.

Delamination of Fe_2AlB_2 in molten salts

Classical delamination of Fe_2AlB_2 by aqueous acidic washing either completely dissolves Fe_2AlB_2, or does not show major structural changes. Alternative delamination paths were then explored. We proposed the use of the molten-salts delamination method published by M. Li[5] and Y. Li[6] for MAX phases. According to this approach, the Al atoms could be selectively oxidized by a molten salt (MCl_2) according to **Equation 3**.

$$2\ Fe_2AlB_2(s) + 3\ MCl_2(l) \rightarrow 2\ Fe_2B_2(s) + 3\ M(s) + 2\ AlCl_3(g)\uparrow \qquad \textbf{Equation 3}$$

Following the guidelines offered by Y. Li with respect to the choice of the delaminating salt, Co^{2+}, Fe^{2+}, Cd^{2+}, and Zn^{2+} would provide sufficiently elevated electrochemical potentials to trigger Al oxidation. We explored all four of them, in the forms of eutectic mixtures with NaCl in order to lower their melting point: $CoCl_2$ (from 798 to 359 °C), $FeCl_2$ (from 671 to 372 °C), $CdCl_2$ (from 564 to 325 °C) and $ZnCl_2$ (from 313 to 249 °C).[7] The mixtures were prepared such that they yield the Fe_2AlB_2:MCl_2 (M = divalent cation) ratio of 2:3 and these were heated only up to 600 °C in order to avoid the decomposition of Fe_2AlB_2. The results of the *in situ* scans are shown in **Figure 4**.

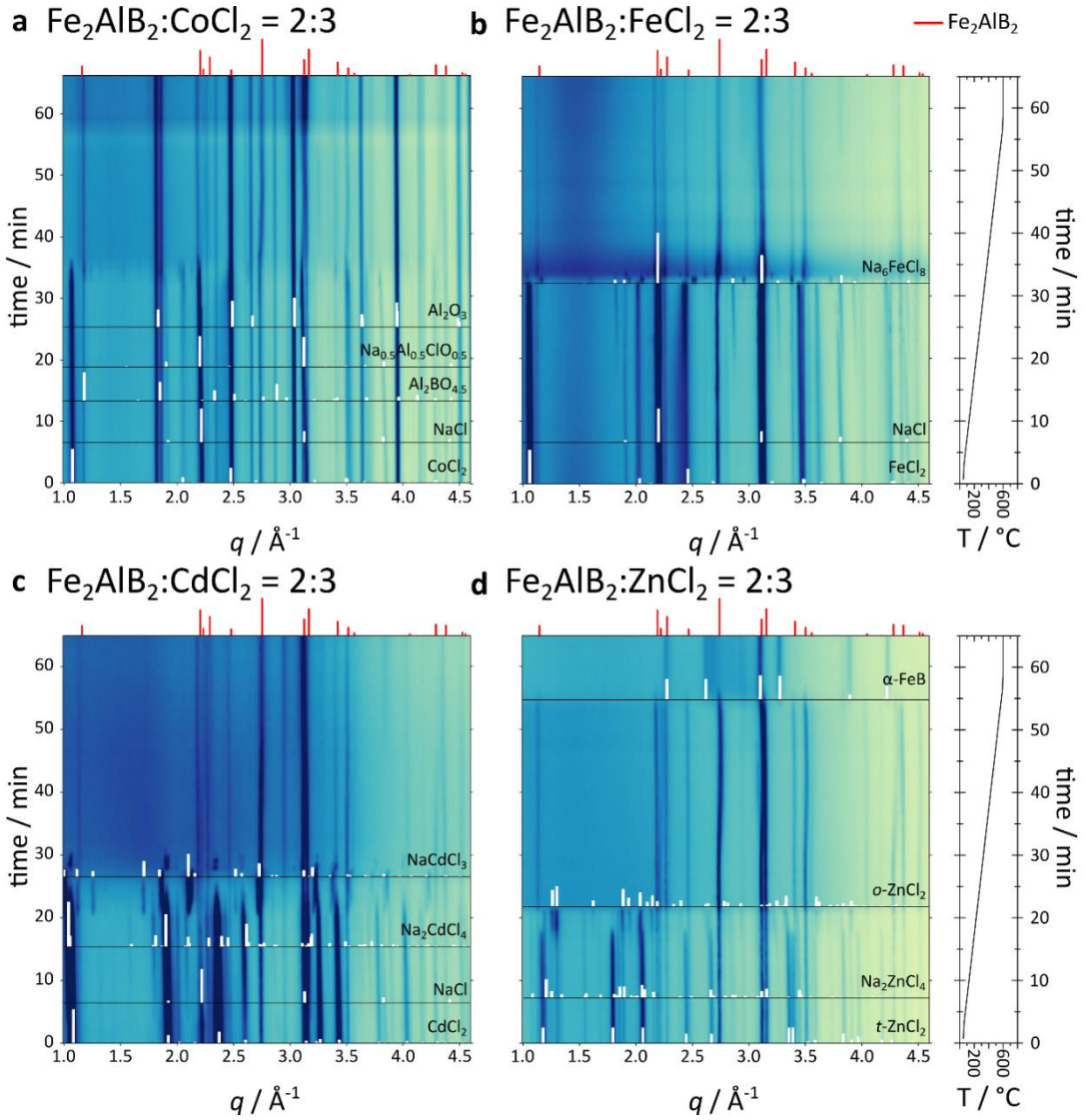

Figure 4. *In situ* XRD study of Fe_2AlB_2 delamination attempts with MCl_2/NaCl eutectic salts in Fe_2AlB_2:MCl_2 ratio of 2:3 for M = Co **(a)**, Fe **(b)**, Cd **(c)**, Zn **(d)**.

Some of the mixtures proved reactive even before the heating, so during the ball-milling process to homogenize the mixtures. For instance, $CoCl_2$ may have contained moisture from the start, as the initial mixture reacted to form Al_2O_3, $Na_{0.5}Al_{0.5}ClO_{0.5}$ and $Al_2BO_{4.5}$. Also, $ZnCl_2$ reacted at room temperature with NaCl to form Na_2ZnCl_4, to the point where NaCl is not detected at all. Other salt mixtures form stoichiometric compounds upon heating, like $FeCl_2$ + 6NaCl → Na_6FeCl_8, $CdCl_2$ + 2NaCl → Na_2CdCl_4, Na_2CdCl_4 + $CdCl_2$ → 2$NaCdCl_3$ or even $ZnCl_2$ showing a phase transition from tetragonal (*t*-$ZnCl_2$) to orthorhombic $ZnCl_2$ (*o*-$ZnCl_2$). In any case, these transformations occur at relatively low temperature and before the melting point. Once this is achieved, none of the mixtures showed evidence of delaminating Fe_2AlB_2. This is observed by following the (020) peak of Fe_2AlB_2 at q = 1.14 $Å^{-1}$, which corresponds the stacked Fe_2B_2 and Al layers in the title compound. We did not observe any significant shift of this peak in any of the experiments.

Still, we observed an unexpected behavior. Beyond 400 °C, certain Bragg peaks from the Fe_2AlB_2 phase begin to shift to higher q values while the temperature is increasing, contrary to what would be expected from conventional thermal expansion. This denotes an anisotropic shrinkage. This result comes as surprising, since this is not in agreement with previous reports, which indicate that Fe_2AlB_2 is stable under argon up to at least 1200 °C[8], or decomposes directly to FeB (depending on the synthetic origin of the compound).[9–11] No abnormal lattice shrinkage has been observed previously. This observation raised the question of the origin of this counterintuitive structural change. The thermal behaviour of Fe_2AlB_2 is studied in the literature, for which a conventional positive expansion coefficient is reported, so we do not expect negative thermal expansion to be at the origin of this observation.[9] Instead, another way a structure can shrink is through the expulsion of atoms out of the structure. In our case, this behaviour would hint to the possibility of delamination by sublimation of Al. In order to identify the origin of this possible atom lost, we performed a blank experiment. The same heating program was reproduced for the isolated Fe_2AlB_2 compound, the results are depicted in **Figure 5**. The same shrinking tendency is observed, indicating that the molten salts and other reagents are not at the origin of the possible element loss of the structure.

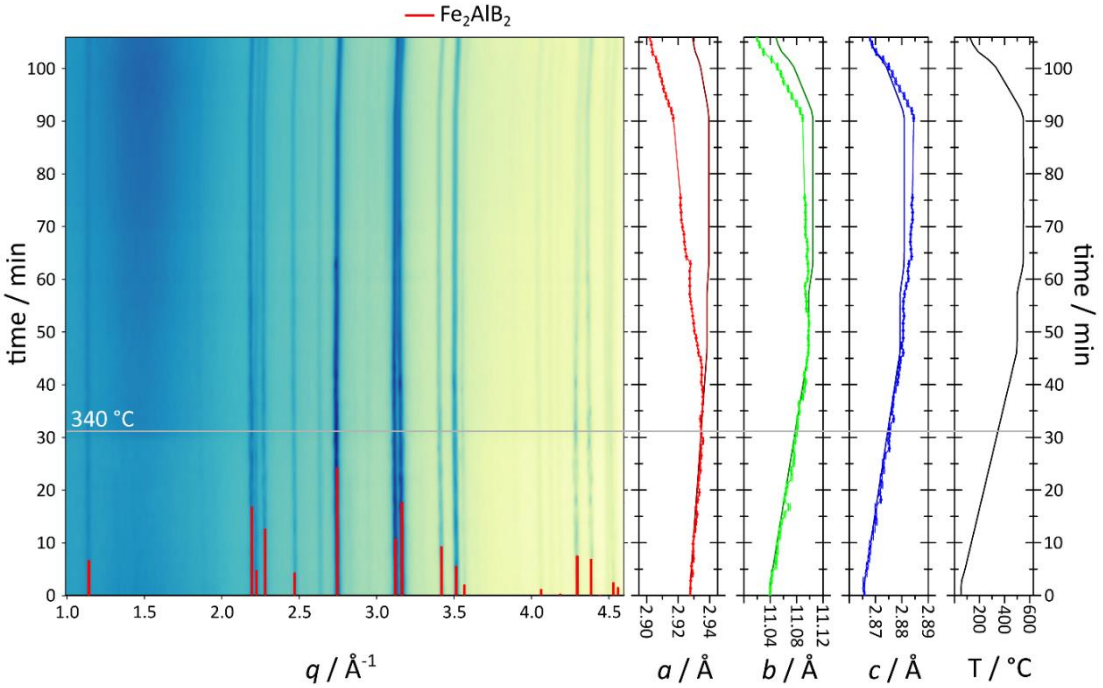

Figure 5. *In situ* XRD study of Fe_2AlB_2 along with the empirical temperature profiles and the refined lattice parameters from sequential Rietveld refinement. In each lattice parameter plot, the refined parameters are plotted as a scatter + line, and compared to the lattice parameters expected from thermal expansion in straight line.

In light of the systematic observation of the lattice shrinkage, we decided to characterize more deeply this anomalous structural collapse. We followed the structural changes against temperature by performing sequential Rietveld refinements for all the diagrams. The results are plotted in **Figure 5**. The refined length of the *a*, *b* and *c* axis are plotted in comparison to the expected length according to the empirical linear anisotropic thermal expansion coefficients –$\alpha_a = 8.1(1)\cdot10^{-6}$ K^{-1}, $\alpha_b = 11.9(2)\cdot10^{-6}$ K^{-1}, $\alpha_c = 10.7(3)\cdot10^{-6}$ K^{-1}–.[9] Indeed, the refinement confirms that the *a* lattice parameter shrinks above 340 °C. We observed that the shrinkage is not reversible, thus confirming the hypothesis that negative thermal expansion is not responsible for the underlying phenomena. Interestingly, the *b* axis also shrinks to a certain extent, although not as much as the *a parameter*, which by the end of the thermal treatment is contracted by a 0.93 %. The *c* axis seems to expand beyond the thermal expansion prediction, but this is explained by the fact that thermal expansion coefficients for Fe_2AlB_2 actually increase with temperature.[12] The used value of the thermal expansion coefficient is a mean value suitable only up to 500 °C, so it can be expected that for higher temperatures this will increase and consequently expand the lattice at a higher rate, but the anisotropic α is not experimentally reported beyond that temperature range. The strongest hypothesis at this point is that certain elements are expulsed from the structure.

In parallel to the experiment depicted in **Figure 5**, we also collected the diffraction patterns at 5 mm above the sample position, which is a colder spot where eventually, the expelled atoms could deposit. Indeed, we detected the appearance of a crystalline phase at the same time as Fe_2AlB_2 begins to contract, as shown in **Figure 6**. This phase corresponds to iron fcc, although not in the standard lattice parameter metrics of 3.648 Å, instead, the diagram matches better a smaller lattice parameter of 3.544 Å, suggesting that this Fe phase is partially substituted by a smaller element. So indeed Fe is expelled along with another element, most likely boron as its atomic radius of 85 pm is smaller than that of Fe (126 pm) while that is not the case for Al (143 pm).[13]

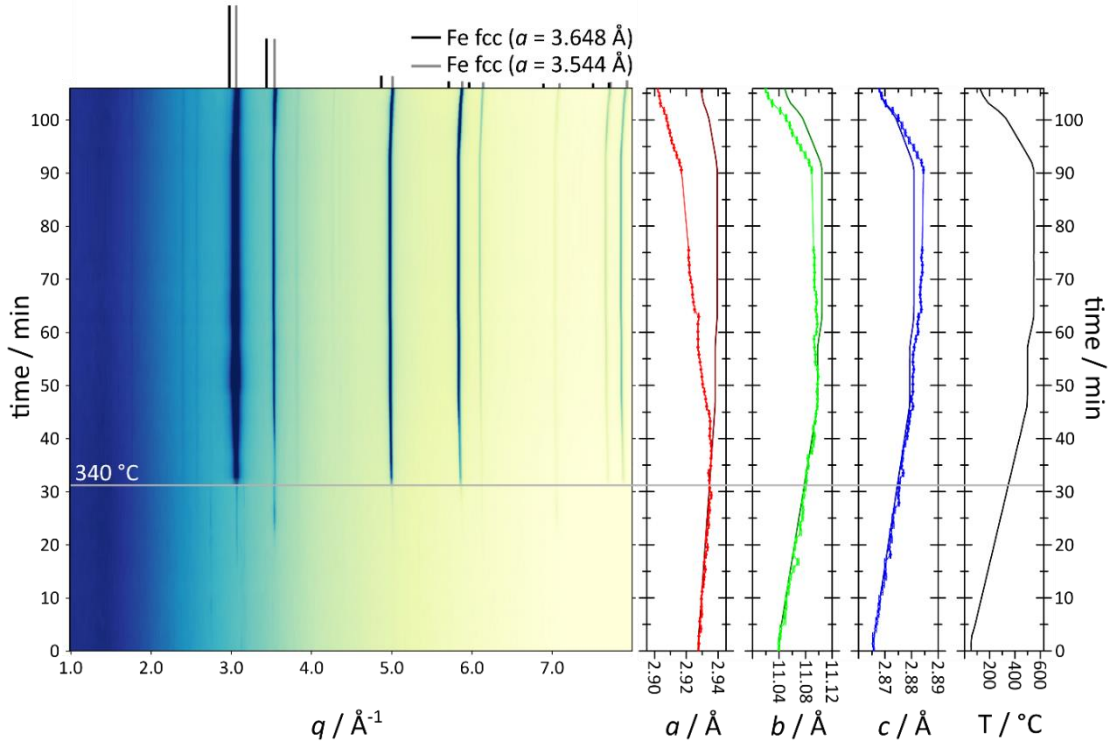

Figure 6. *In situ* XRD of Fe_2AlB_2 thermal treatment probing 5 mm above the sample position. The refined lattice parameters and empirical temperature profiles for Fe_2AlB_2 in this experiment are also depicted for comparison.

To further question the nature of the structural change on Fe_2AlB_2, we performed an experiment up to 1000 °C to trigger full decomposition. Interestingly, above 900 °C a phase of stoichiometry $Fe_3Al_2B_2$ begins to form, as shown in **Figure 7**. To characterize the transformation, we also performed sequential Rietveld refinement for the whole dataset, paying special attention to the phase fraction distribution throughout the heat treatment. By doing so, it can be seen that $Fe_3Al_2B_2$ forms at the expense of Fe_2AlB_2, which most likely reacts to yield $Fe_3Al_2B_2$. It can also be observed that Fe (fcc) forms upon this transformation, in line with the previous results on the lower temperature transformation. A possible equation for the transformation could be the one described in **Equation 4**. This chemical equation would explain the detection of Fe as a by-product, and the fact that it possesses smaller lattice parameters than conventional Fe fcc, as it would be partially substituted by boron atoms, also expelled from the structure .

$$2Fe_2AlB_2(s) \rightarrow Fe_3A_2lB_2(s) + FeB_\delta + (2-\delta)B(s) \qquad \textbf{Equation 4}$$

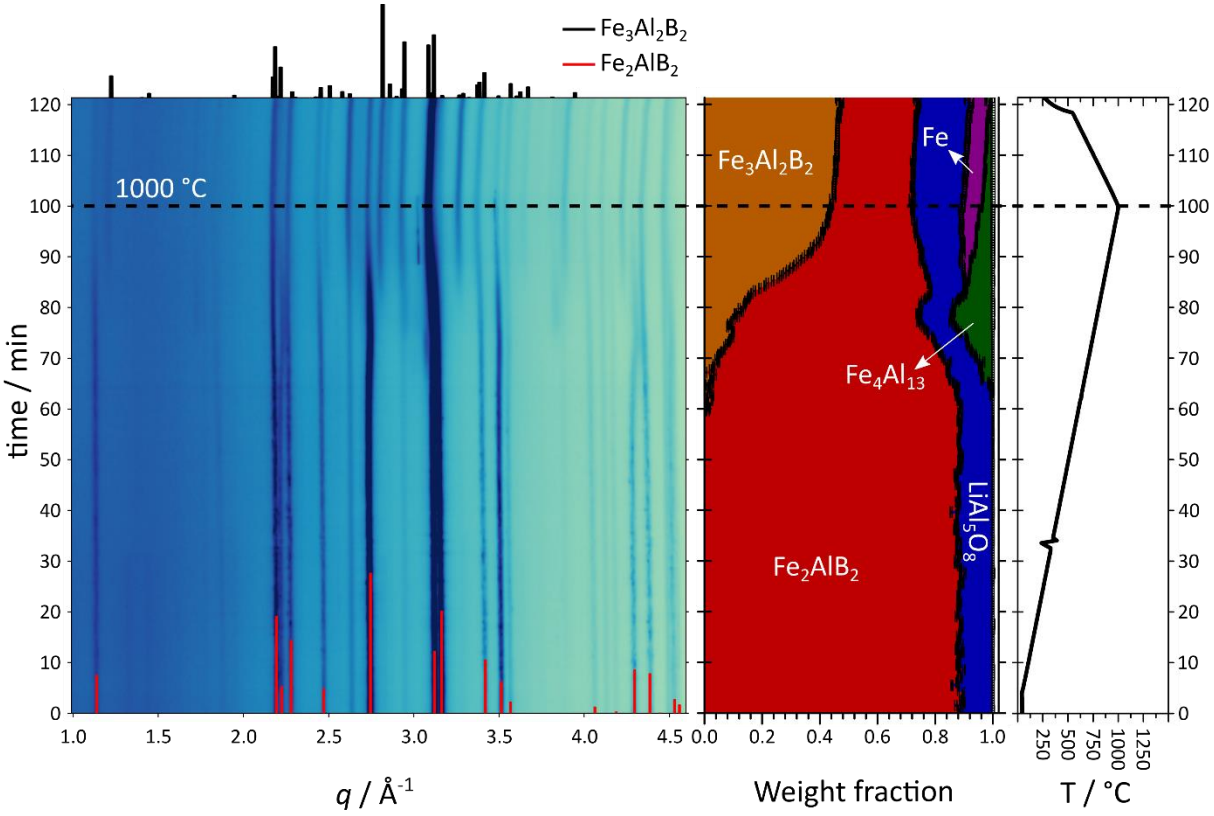

Figure 7. *In situ* XRD study of Fe_2AlB_2 thermal treatment up to 1000 °C along with the empirical temperature profiles and the refined phase fraction against time from sequential Rietveld refinement.

It is interesting to compare the Fe_2AlB_2 and $Fe_3Al_2B_2$ structures to assess the possibility that **Equation 4** would occur. As we have already discussed previously, Fe_2AlB_2 consists of infinite layers of Fe_2B_2 (**Figure 8a**), stacked along the *b* axis and separated by a layer of Al atoms. Each Fe_2B_2 layer contains zig-zag B chains, coordinated to Fe atoms lying to the exterior of the layers. $Fe_3Al_2B_2$ on the other hand contains isolated portions of the Fe_2B_2 layers that extend to only 4 B atoms chain-length, as highlighted in **Figure 8b**. These unities are not aligned as if they continued the layers in Fe_2AlB_2, but instead they are shifted out-of-plane. In order to Fe_2AlB_2 into $Fe_3Al_2B_2$, firstly the layers must be cut every other Fe_2B_4 moiety as marked in **Figure 8a** in yellow. Eliminating such portions already yields the final stoichiometry, but the remaining portions must still follow the movement marked with red arrows in **Figure 8a** in order to reproduce the mismatch from the $Fe_3Al_2B_2$ structure. This movement also affects

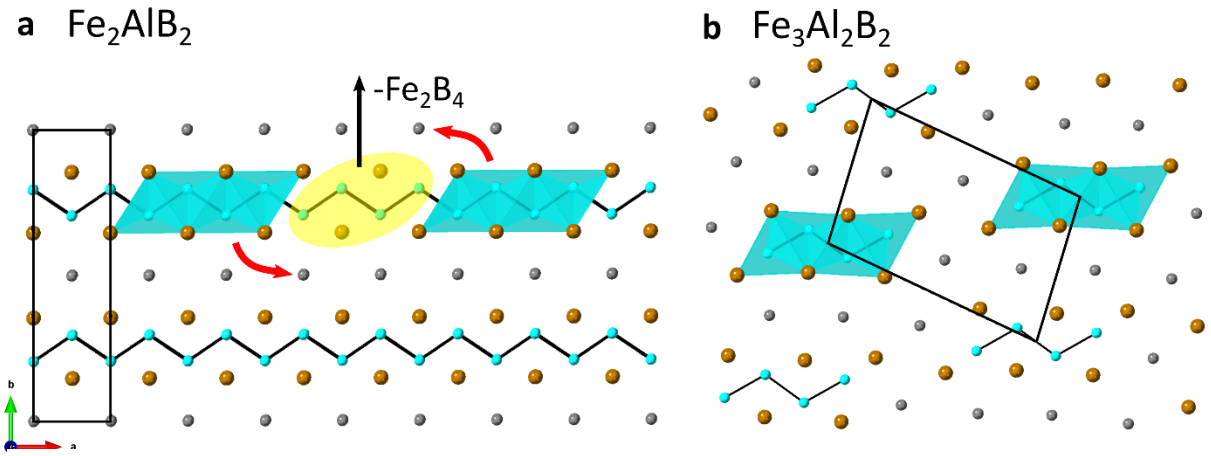

Figure 8. Comparison of structures of Fe_2AlB_2 **(a)** and $Fe_3Al_2B_2$ **(b)**.

mostly the distances in the *a* direction of Fe_2AlB_2, by contracting *a* while leaving *b* and *c* practically unaltered. This movement would in fact explain the repeatedly observed shrinkage of Fe_2AlB_2 in the *a* direction, as characterized in the experiment of **Figure 6**. The observed shrinkage of the *a* lattice parameter would indicate a transient state between Fe_2AlB_2 and $Fe_3Al_2B_2$, where Fe-B vacancies are being generated, which can exist up to a certain extent but ultimately leads to the transition towards $Fe_3Al_2B_2$.

Conclusions

The *in situ* studies were performed thanks to the development of a synchrotron sample environment that permits to work in inert conditions. We studied the synthesis and delamination of Fe_2AlB_2 and derived compounds. The synthesis of this phase was achieved in molten salts by using α-FeB as starting material. Al could be inserted inside the α-FeB structure. Al formation as an intermediate product was confirmed by *in situ* X-ray diffraction. The sequence of reactions was also shown to be identical for the α and β-FeB polymorphs as starting materials. We then explored the exfoliation of Fe_2AlB_2 with molten salts. The salts did not prove major reactivity. However, Fe_2AlB_2 exhibited an abnormal lattice contraction with the temperature, which was associated to the formation of Fe/B vacancies that ultimately lead to a transformation to the $Fe_3Al_2B_2$ compound beyond 900 °C. This abnormal thermal behaviour has not been reported previously in the literature and can could only be identified thanks to the *in situ* monitoring of the reaction. Interestingly, the resulting defectuous compounds would hold a large content of vacancies, which may deeply impact catalytic properties, enable tailoring the physical properties of Fe_2AlB_2-based materials and possibly assist the exfoliation process. Further studies on this manner are ongoing.

References:

[1]: L. T. Alameda, P. Moradifar, Z. P. Metzger, N. Alem and R. E. Schaak, *J. Am. Chem. Soc.*, 2018, **140**, 8833–8840.

[2]: Z. Guo and Z. Sun, *J. Mater. Chem. A*, 2017, **5**, 23530–23535.

[3]: J. Zhou, J. Palisaitis, J. Halim, M. Dahlqvist, Q. Tao, I. Persson, L. Hultman, P. O. Å. Persson. and J. Rosen, *Science (80-.).*, 2021, **373**, 801–805.

[4]: B. Anasori, M. R. Lukatskaya and Y. Gogotsi, *Nat. Rev. Mater.*, 2017, **2**, 16098.

[5]: M. Li, J. Lu, K. Luo, Y. Li, K. Chang, K. Chen, J. Zhou, J. Rosen, L. Hultman, P. Eklund, P. O. Å. Persson, S. Du, Z. Chai, Z. Huang and Q. Huang, *J. Am. Chem. Soc.*, 2019, **141**, 4730–4737.

[6]: Y. Li, H. Shao, Z. Lin, J. Lu, L. Liu, B. Duployer, P. O. Å. Persson, P. Eklund, L. Hultman, M. Li, K. Chen, X. H. Zha, S. Du, P. Rozier, Z. Chai, E. Raymundo-Piñero, P. L. Taberna, P. Simon and Q. Huang, *Nat. Mater.*, 2020, **19**, 894–899.

[7]: www.crct.polymtl.ca/fact/documentation/FTsalt/FTsalt_Figs.htm (Revised on the 05/08/2022).

[8]: E. M. Levin, B. A. Jensen, R. Barua, B. Lejeune, A. Howard, R. W. McCallum, M. J. Kramer and L. H. Lewis, *Phys. Rev. Mater.*, 2018, **2**, 34403.

[9]: L. Verger, S. Kota, H. Roussel, T. Ouisse and M. W. Barsoum, *J. Appl. Phys.*, , DOI:10.1063/1.5054379.

[10]: S. Kota, L. Verger, V. Natu, M. Sokol and M. W. Barsoum, *J. Am. Ceram. Soc.*, 2021, **104**, 733–739.

[11]: J. Liu, S. Li, B. Yao, J. Zhang, X. Lu and Y. Zhou, *Ceram. Int.*, 2018, **44**, 16035–16039.

[12]: Y. Bai, X. Qi, X. He, G. Song, Y. Zheng, B. Hao, H. Yin, J. Gao and A. Ian Duff, *J. Am. Ceram. Soc.*, 2020, **103**, 5837–5851.

[13]: J. C. Slater, *J. Chem. Phys.*, 1964, **41**, 3199–3204.